Tubular Flow Photoreactors for Complex, Nonchain Kinetics

YOSHIO HARANO and J. M. SMITH

University of California, Davis, California

The stationary state hypothesis, commonly used for intermediates in complex kinetics in batch reactor studies, is analyzed in a tubular flow photoreactor. For practical values of the rate constants for the chosen kinetic sequence, it appears that the hypothesis is valid over all but a short entrance region of the reactor for both streamline and plug flow models. Even though the stationary state is quickly achieved, for the normal range of diffusivities, the conversion to product may be affected by radial diffusion and velocity profiles.

In the course of the analysis the pertinent dimensionless parameters establishing the behavior of the reactor were identified. These arose from the differential equations expressing the conservation of radiant energy and mass in the system.

In an earlier paper (*6*) kinetic constants for the photochlorination of propane were evaluated from data obtained in a laboratory scale, flow reactor. By differential reactor operation with small concentrations of reactants it was possible to circumvent most of the complexities associated with photoreactors. In a tubular flow reactor these complexities are due to diffusion and complex kinetics. The variation in light intensity with radial position causes variation in the rate of the initiation step, and this gives rise to radial concentration gradients and diffusion, even for a plug flow reactor. The difficulties due to complex kinetics can be avoided by the stationary state hypothesis for reaction intermediates. However, the conditions for which this is a suitable approximation have not been established. In this paper the effects of diffusion and complex kinetics upon the conversion are analyzed for a relatively simple sequence of reactions. The results, particularly the identification of parameters measuring the importance of diffusion and the stationary state assumption, should be generally valuable. Also, the limiting values of the parameters for which simplified design procedures are adequate provides a guide for cases involving more complicated reaction sequences.

The validity of the stationary state hypothesis apparently has not been studied in a flow reactor, although Benson (*2*) has discussed its suitability for batch conditions. In a valuable contribution Hill and Felder (*12*) have considered effects of three degrees of mixing: 1. no mixing, 2. complete radial but no axial mixing, and 3. complete mixing for slab, cylindrical, and annular reactors. The main assumptions were low conversions and stationary state kinetics. The first assumption limits the results to near differential reactor operation or low conversion per pass. Both assumptions imply either a constant attenuation coefficient, or very small absorptivity so that the attenuation coefficient, $\mu = \alpha C$, approaches zero.

In the analysis that follows the incident light is directed radially into the tubular reactor under the following conditions:

1. Monochromatic light. If the quantum yield for the initiation step is not dependent upon wave length, polychromatic light could be treated by summing the contributions to the light absorbed over the range of wave length involved.
2. Isothermal conditions. This assumption is not likely to be severe, since activation energies for photochemical reactions are normally small.
3. Constant intensity at the wall.
4. Constant absorptivity, α.
5. No dark reaction.
6. Negligible axial diffusion.
7. No wall reaction.
8. Negligible reflection of light at the reactor wall.
9. Constant pressure (for a gaseous reaction).

The chosen reaction sequence involves absorption of light by reactant A and subsequent reaction of the activated molecule or atom to produce product B. The activated form of A can also be destroyed by a first-order termination step, for example, by collision with an inert component M present in constant concentration. By choosing the rate constant for this step to be zero, results for the irreversible formation of activated A are obtainable. The reactions and the local rates of formation of each component are

$$A + h\nu \xrightarrow{\varphi^{\alpha_A I}} A^*$$

$$A^* \xrightarrow{k_2} B$$

$$A^* + M \xrightarrow{k_3 = k_3'(C_M)} A + M$$

where φ is the quantum yield for the initiation reaction and k_2 and k_3 are first-order rate constants. Thus

$$\Omega_{A^*} = -(k_2 + k_3)\, C_{A^*}(r,z) + \varphi\alpha\, I(r,z)\, C_A(r,z) \quad (1)$$

$$\Omega_A = -\varphi\alpha\, I(r,z)\, C_A(r,z) + k_3\, C_A \quad (2)$$

$$\Omega_B = k_2\, C_{A^*}(r,z) \quad (3)$$

The solution required is the conversion of A to B at the exit of the reactor. To accomplish the stated objectives four cases need to be considered: Case I. General solution, Case II. Plug flow (no radial velocity gradient), Case III. No radial concentration gradient, and Case IV. No radial concentration gradient and stationary state hypothesis.

The equations of Case IV, and special forms of Case III, could be solved analytically, while the remainder require numerical solution. The problem is defined by a radiation equation (conservation of radiant energy), mass conservation expressions for each species, and the appropriate boundary conditions. The mass conservation expressions are given for each case in later sections. The radiation equation for cylindrical geometry is developed next.

RADIATION EQUATION FOR A CYLINDRICAL TUBE

Figure 1*a* shows the geometry of the system with two beams of radiation of intensity I_r and I_{R+r} at any radial position r. Conservation of radiant energy applied to this

situation gives

$$\left.\begin{aligned}\frac{1}{r}\frac{\partial}{\partial r}(I_r r) &= \alpha\, C_A(r,z)\, I_r \\ \frac{1}{r}\frac{\partial}{\partial r}(I_{R+r} r) &= -\alpha\, C_A(r,z)\, I_{R+r}\end{aligned}\right\} \quad (4)$$

The total intensity $I(r,z)$ from both beams is needed in Equation (1). By integrating Equation (4) this becomes

$$I(r,z) = \frac{2I_o R}{r}\left[\exp\left(-\alpha_A \int_o^R C_A(r',z)dr'\right)\right]\cosh\left[\alpha_A \int_o^r C_A(r',z)dr'\right] \quad (5)$$

where I_o is the intensity at the inside wall surface from one direction. Equation (5) is applicable for solution of Cases I and II.

No Radial Concentration Gradient

Now $C_A(r,z) = C_A(z)$, and the integrals in Equation (5) can be evaluated, giving

$$I(r) = \frac{2I_o R}{r}\left[\exp\left(-\alpha_A C_A(z)\, R\right)\right]\cosh\left(\alpha_A C_A(z)\, r\right) \quad (6)$$

The intensity is still a function of r. However the rate of the initiation step is first order in $I(r)$, according to Equation (1), so that an average intensity $\overline{I}$ across the tube can be used to obtain the average rate of the initiation step. Integrating Equation (6) and dividing by the area gives

$$\overline{I} = \frac{2\, I_o}{R\,\alpha_A C_A(z)}\left[-\exp\left(-2\alpha_A C_A(z)\, R\right)\right] \quad (7)$$

Equation (7) is applicable for Cases III and IV.

Special Situations

If the conversion is low, $C_A(z)$ will be approximately constant. Then the intensity equation [Equation (6)] will not be coupled with the mass balance expressions and can be written in terms of a constant attenuation coefficient $\mu = \alpha\, C$ as follows:

$$I(r) = \frac{I_o R}{r}\left[e^{-\mu(R-r)} + e^{\mu(R+r)}\right] \quad (8)$$

This equation has been used widely, but it should be noted that it is only applicable when μ is constant.

If the absorptivity is very low, Equations (6) and (7) reduce to the simple forms:

$$I(r) = \frac{2R\, I_o}{r} \quad (9)$$

$$\overline{I} = 4\, I_o \quad (10)$$

CASE I

For laminar flow in the reactor (Figure 1) the mass balance of species i is

$$-2\bar{v}\left[1-\left(\frac{r}{R}\right)^2\right]\frac{\partial C_i}{\partial z} + D_i\left[\frac{1}{r_i}\frac{\partial}{\partial r}\left(r\frac{\partial C_i}{\partial r}\right)\right] + \Omega_i = 0 \quad (11)$$

The choice of laminar flow will create the greatest deviation from plug flow behavior. At the reactor inlet suppose C_{A^*} and C_B are zero and $C_A(r,o) = C_{A_o}$. With no wall reactions the concentration gradient of each species at the wall will be zero. At the axis the boundary condition is given by the method of Schechter and Wissler (*16*); that

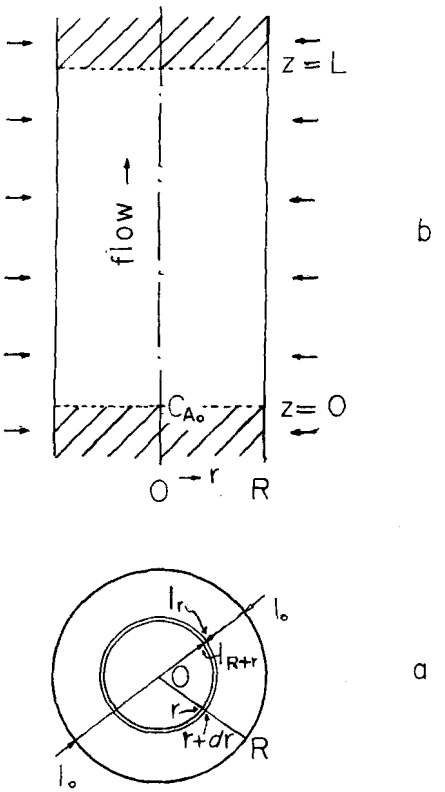

Fig. 1. Reactor geometry.

is

$$\left(\frac{\partial C_i}{\partial r}\right)_{r=0} = \lim_{r\to 0}\frac{1}{D_i r}\int_o^r \Omega_i\, r'\, dr' \quad (12)$$

This form is necessary because the intensity approaches infinity at the axis [Equation (5)] but the volume for reaction approaches zero. The rate for component B is not a function of $I(r)$ so the right side of Equation (12), when applied to B, is zero. For A^* and A the limit form must be used.

By writing Equations (11) and (12) in dimensionless form with the independent variables

$$\rho = r/R \quad (13)$$

$$\zeta = z/L \quad (14)$$

$$\theta = zd/\bar{v} = \theta_o\zeta \quad (15)$$

indicates that the following parameters are needed:

$$d = k_2 + k_3 \quad (16)$$

$$\theta_o = \tau_o d = \frac{L}{\bar{v}}d \quad (17)$$

$$\epsilon_o = RC_{A_o}\alpha_A \quad (18)$$

$$\kappa = \varphi\alpha_A I_o \quad (19)$$

$$M_i = D_i/R^2 d \quad (20)$$

$$a = k_2/d \quad (21)$$

$$b = \kappa/d \quad (22)$$

Here $2\epsilon_o$ is the optical thickness at the reactor inlet, τ_o the mean residence time, and κ the equivalent first-order rate constant for the initiation step, evaluated at the wall intensity. If the dimensionless, dependent variables are

$$X = C_{A^*}/C_{A_o} \quad (23)$$

$$Y = C_A/C_{A_o} \quad (24)$$

$$Z = C_B/C_{A_o} \quad (25)$$

the three mass balance equations may be written

$$2(1-\rho^2)\frac{\partial X}{\partial \theta} - M_{A^*}\left(\frac{1}{\rho}\frac{\partial X}{\partial \rho} + \frac{\partial^2 X}{\partial \rho^2}\right) + X - \frac{2b}{\rho} Y\left[\exp\left(-\epsilon_o \int_o^1 Y\, d\rho'\right)\right] \cosh\left[\epsilon_o \int_o^\rho Y\, d\rho'\right] = 0 \quad (26)$$

$$2(1-\rho^2)\frac{dY}{d\theta} - M_A\left(\frac{1}{\rho}\frac{\partial Y}{\partial \rho} + \frac{\partial^2 Y}{\partial \rho^2}\right) - (1-a)X + \frac{2b}{\rho} Y\left[\exp\left(-\epsilon_o \int_o^1 Y\, d\rho'\right)\right] \cosh\left[\epsilon_o \int_o^\rho Y\, d\rho'\right] = 0 \quad (27)$$

$$2(1-\rho^2)\frac{\partial Z}{\partial \theta} - M_B\left(\frac{1}{\rho}\frac{\partial Z}{\partial \rho} + \frac{\partial^2 Z}{\partial \rho^2}\right) - aX = 0 \quad (28)$$

The boundary conditions are

$$X(\rho,o) = 0;\ Y(\rho,o) = 1;\ Z(\rho,o) = 0 \quad (29)$$

$$\left(\frac{\partial X}{\partial \rho}\right)_{1,\zeta} = \left(\frac{\partial Y}{\partial \rho}\right)_{1,\zeta} = \left(\frac{\partial Z}{\partial \rho}\right)_{1,\zeta} = 0 \quad (30)$$

$$\left(\frac{\partial X}{\partial \rho}\right)_{0,\zeta} = -\frac{2b}{M_{A^*}} Y\left[\exp\left(-\epsilon_o \int_o^1 Y\, d\rho'\right)\right] \cosh\left[\epsilon_o \int_o^\rho Y d\rho'\right] \quad (31)$$

$$\left(\frac{\partial Y}{\partial \rho}\right)_{0,\zeta} = \frac{2b}{M_A} Y\left[\exp\left(-\epsilon_o \int_o^1 Y d\rho'\right)\right] \cosh\left[\epsilon_o \int_o^\rho Y d\rho'\right] \quad (32)$$

$$\left(\frac{\partial Z}{\partial \rho}\right)_{0,\zeta} = 0 \quad (33)$$

Equations (31) to (33) were obtained from Equation (12) by applying L'Hopital's rule.

Equations (26) to (28) were written in difference form, using the implicit method (*8, 14*) for the second term, and the explicit method for the first term and the reaction terms. The equations were solved numerically using the Thomas method (*4, 14*). The stability and convergence of the solution would be improved by using the implicit form for the reaction terms, as was done by Cleland and Wilhelm (*7*) for a single partial differential equation. This approach is not suitable for this case where three equations must be solved simultaneously. To check the approach we used, both methods were applied to an artificial problem where but one equation of the form of Equation (26) was involved. The two methods gave results for X which agreed within 0.2%.

It was assumed that the diffusivities of all the components were equal, so but one value of M was needed. Summation of Equations (26) to (28) for this case requires that $X + Y + Z = 1.0$. This property was used to check the numerical results. The mean concentrations were evaluated by integration across the diameter of the reactor; for example, for X we obtain

$$\overline{X} = 4\int_o^1 X(\rho)\,\rho(1-\rho^2)\,d\rho \quad (34)$$

CASE II. PLUG FLOW

In a conventional isothermal reactor the radial diffusion term in the balance disappears for plug flow conditions. In a photoreactor this is not the case because of the variation in light intensity with radial position. Hence the only simplification in Equation (11) for plug flow is that $v = \overline{v}$. In dimensionless form the resulting three mass balances are identical to Equations (26) to (28) except the coefficient, $2(1-\rho^2)$, of the first term disappears in each case. Equations (29) to (33) for the boundary conditions are unchanged.

The same general numerical techniques were used for this case. Convergent solutions were obtained more rapidly than for Case I. The sum of the dimensionless concentrations was close to unity for all solutions, the maximum difference being 0.06%. The average concentrations at any reactor length were evaluated, for example, X, from the following integral:

$$\overline{X} = 2\int_o^1 X(\rho)\,\rho\,d\rho \quad (35)$$

CASE III. NO RADIAL CONCENTRATION GRADIENT

The premise here is that radial diffusion is rapid with respect to reaction and convective flow so that $M_i = \infty$. Since the rates are first-order, a velocity profile for this case has no effect on the average concentrations. Benson (*2*) has considered situations similar to this case and also to Case IV. The three mass balance equations are those of Case II with $M_i = \infty$ and $C_i(r,z) = C_i(z)$. They may be written:

$$\frac{dX}{d\theta} + X - \frac{2b}{\epsilon_o}(1 - e^{-2\epsilon_o Y}) = 0 \quad (36)$$

$$\frac{dY}{d\theta} - (1-a)X + \frac{2b}{\epsilon_o}(1 - e^{-2\epsilon_o Y}) = 0 \quad (37)$$

$$\frac{dZ}{d\theta} - aX = 0 \quad (38)$$

with the initial conditions

$$X = 0,\ Y = 1,\ Z = 0 \text{ at } \zeta = 0 \quad (39)$$

Equations (36) to (38) are a set of nonlinear, coupled, ordinary differential equations. The set does not appear to be solvable analytically so a numerical solution was obtained using the Runge-Kutta-Gill method (*14*). The reliability of the method was checked by comparison with the analytical solution of Equation (37) for $a = 1$.

Low Optical Thickness Case (IIIa)

Since in some photochemical reactions ϵ_o will approach zero, the equations for $\epsilon_o \to 0$ define an important special case. Equations (36) to (39) become:

$$\frac{dX}{d\theta} + X - 4bY = 0 \quad (40)$$

$$\frac{dY}{d\theta} - (1-a)X + 4bY = 0 \quad (41)$$

$$\frac{dZ}{d\theta} - aX = 0 \quad (42)$$

This set can be solved analytically to give

$$X = \frac{8b}{\Phi_1 - \Phi_2}\left[\exp-(-\Phi_1\theta/2) + \exp(-\Phi_2\theta/2)\right] \quad (43)$$

$$Y = \frac{1}{\Phi_1 - \Phi_2}[-(\Phi_2 - 8b)\exp(-\Phi_1\theta/2) + (\Phi_1 - 8b)\exp(-\Phi_2\theta/2)] \quad (44)$$

$$Z = 1 + \frac{1}{\Phi_1 - \Phi_2}[\Phi_2 \exp(-\Phi_1\theta/2) - \Phi_1 \exp(-_2\theta/2)] \quad (45)$$

where

$$\Phi_1 = (4b + 1) + [(4b + 1)^2 - 16ab]^{1/2} \quad (46)$$

$$\Phi_2 = (4b + 1) - [(4b + 1)^2 - 16ab]^{1/2} \quad (47)$$

These results show that the performance of the reactor is determined by three parameters: $\theta_o = \tau_o(k_2 + k_3)$; $b = \varphi\alpha_A I_o/(k_2 + k_3)$; and $ab = \dfrac{k_2(\varphi\alpha_A I_o)}{(k_2 + k_3)^2}$. For $\epsilon_o \leq 10^{-4}$ the numerical solution of Equations (36) to (39) was nearly the same as the analytical result from Equations (43) to (45).

CASE IV. STATIONARY STATE KINETICS AND NO RADIAL CONCENTRATION GRADIENT

According to the Stationary State hypothesis the concentrations of intermediate, unstable species (A^* in our system) are negligible with respect to the concentrations of the stable components. If stoichiometric relations hold, this hypothesis also means that the rate of reaction for the unstable species is essentially zero, or $dX/d\theta = 0$ for our system. Applied to Case III, Equations (36) to (39) reduce to

$$X = \frac{2b}{\epsilon_o}(1 - e^{-2\epsilon_o Y}) \to 0 \quad (48)$$

$$\frac{dY}{d\theta} = \frac{2ab}{\epsilon_o}(1 - e^{-2\epsilon_o Y}) \quad (49)$$

$$\frac{dZ}{d\theta} = -\frac{2ab}{\epsilon_o}(1 - e^{-2\epsilon_o Y}) \quad (50)$$

The analytical solution is straightforward giving

$$X = \frac{2b}{\epsilon_o}\{1 - [1 + (e^{2\epsilon_o} - 1)\, e^{-4ab\theta}]^{-1}\} \to 0 \quad (51)$$

$$Y = \frac{1}{2\epsilon_o}\{\ln[1 + (e^{2\epsilon_o} - 1)\, e^{-4ab\theta}]\} \quad (52)$$

and

$$Z = 1 - Y \quad (53)$$

Low Optical Thickness Case (IV*a*)

If $\epsilon_o \to 0$, differential Equations (48) to (50) are simplified still further and lead to the following solution:

$$X = 4b\, e^{-4ab\theta} \to 0 \quad (54)$$

$$Y = e^{-4ab\theta} \quad (55)$$

$$Z = 1 - e^{-4ab\theta} \quad (56)$$

REQUIREMENT FOR STATIONARY STATE HYPOTHESIS

For the concentration of A^* to be low, the rate constants of the reactions for destruction of A^* should be large with respect to the rate constant of the initiation step. A criterion for this is the parameter $b = (\varphi\alpha_A I_o)/(k_2 + k_3)$. It can be shown that Equations (43) to (45) for Case III*a* reduce to Equations (54) to (56) for IV*a* when $b \to 0$. While this reduction cannot be verified analytically when $\epsilon_o \neq 0$, machine computation at successively lower values of b indicated that $b \to 0$ was sufficient for the results of Case III to equal those for Case IV. Hence a necessary and sufficient criterion for the stationary state hypothesis for our reaction system is that $b \to 0$. This means that $X \to 0$ in Equations (48), (51), and (54). For more complex reaction sequences additional, relative rate parameters would need to be defined, but it appears, as Benson pointed out (2), that such parameters constitute a satisfactory requirement for the Stationary State hypothesis. The stationary state hypothesis as defined is a kinetic one. The fact that $b \to 0$ does not mean that radial diffusion is unimportant. To evaluate this effect requires a comparison of Cases I or II and III. Comparison of Cases III and IV establishes the significance of the stationary state hypothesis since no radial gradients exist for either case.

The design parameters that determine the concentration in the reactor are summarized for Cases III and IV in Table 1; a and b are relative rate constants, and θ_o is the product of the average residence time and $(k_2 + k_3)$. The results for stationary state conditions can be represented in terms of two parameters $ab\theta_o$ and ϵ_o, and this reduces to $ab\theta_o$ *if* $\epsilon_o \to 0$.

Table 1. Pertinent Design Parameters (Cases III and IV)

Reactor model	Parameter
III	ϵ_o; a; b; θ_o
III^a($\epsilon_o \to 0$)	b; ab; θ_o
IV	ϵ_o; $ab\theta_o$
IV^a($\epsilon_o \to 0$)	$ab\epsilon_o$

NUMERICAL VALUES OF PARAMETERS

In order to calculate the reactor performance over a practical range of parameter values, it was necessary to estimate rate constants. This was done for the photochemical variables with the aid of information in various references (*1, 3, 5, 6, 9 to 11, 13, 15*).

The range of values for k_2 was estimated by the Rice, Ramsberger and Kassel theory (*1, 3*) for the unimolecular reaction of a hot radical or molecule. The range of wave length λ was chosen to be 4,000- 2,000 Å. (79 to 130 kcal./g. mole), the activation energy for the forward reaction was 25 to 84 kcal./g. mole, the frequency of transfer of energy from one degree of freedom to another was 10^5-10^{17} sec.$^{-1}$, and the number of active degrees of freedom equal to 10. Then k_2 was calculated to be from 10^3 to 10^{12} sec.$^{-1}$. For k_3 the following equation was employed:

$$k_3 = \lambda_D K_{A^*} \quad (33)$$

λ_D is the fraction of the collisions of A^* which result in deactivation; its range was taken as 10^{-3} to 1(1). K_{A^*} is the collision frequency of A^* with inert M. The results for gas and liquid phase systems are given in Part A of Table 2 along with values for the other variables. From the stoichiometry of the reaction, A, A^*, and B all have the same molecular weight. This provides some justification for assuming equal diffusivities for all the species. Without this simplification, separate values of D_i and M_i would be introduced for each component, which would lead to confusion in interpreting the results.

The values of the groups of variables that are significant for design are given in part B of the table. The maximum, practical levels estimated for b and M_i are 10^{-3} and 10^{-4}. In making this estimate for M_i, molecular diffusivities were used. These parameters determine the significance of deviations from the stationary state hypothesis and the importance of radial diffusion. Considering that the estimates may be in error, computer results were also obtained at larger values for these two quantities. Also, for turbulent flow the convective contribution to radial mass transfer

would increase M_i. Turbulent flow conditions would correspond most closely to Case II, with relatively high values of M_i.

TABLE 2. ESTIMATED RANGE OF DESIGN PARAMETERS

A. Variables

R, cm.	10^{-1} -20
C_{A_0}, g.mole/cc.	10^{-7} -10^{5} (gas); 10^{-5} -10^{-3} (liquid)
φ, g.mole/Einstein	0.1 -1
I_0, Einstein/(cm.)^2(sec.)	10^{-11} -10^{-6}
α, cc./(cm.)(g.mole)	10^{3} -10^{6}
k_2, sec.$^{-1}$	10^{3} -10^{12}
k_3, sec.$^{-1}$	10^{8} -10^{11} (gas); 10^{7} -10^{11} (liquid)
κ, sec.$^{-1}$	10^{-9} -1
d, sec.$^{-1}$	10^{3} -10^{12}
D, sq.cm./sec.	10^{-2} -1 (gas); 10^{-5} -10^{-6} (liquid)
τ_0, sec.	10 -10^{2}

B. Design parameters (dimensionless)

$a = k_2/d$	10^{-8} -1
$b = \kappa/d$	10^{-21} -10^{-3}
$\epsilon_0 = R C_{A_0}\alpha$	10^{-5} -10^{4}
$\theta_0 = \tau_0 d$	10^{4} -10^{14}
$ab\theta_0$	10^{-17} -10^{11}
$M = D/R^2 d$	10^{-21} -10^{-4}
$M\theta_0$	10^{-10} -1
$\beta = b\theta_0/\epsilon_0$	10^{-12} -10^{3}

RESULTS AND DISCUSSION

Stationary State Hypothesis

A comparison of the results for Cases III and IV shows the conditions for which the stationary state hypothesis is valid. Table 1 indicates that the comparison should depend upon a, b, and ϵ_0 at a fixed value of $ab\theta_0$. Figure 2 illustrates the results. Here $ab\theta_0$ is unity (which would correspond to reasonably large conversions), $a = 1$, and ϵ_0 and b vary. Of particular interest are the three solid curves for X, (A^*/A_0) vs. reactor length at the bottom of the figure. When b is much less than 10^{-2}, the concentration of A^* will be very small and nearly to that for Case IV ($b \to 0$), which is the horizontal line at 0. The solid curves for Z show similar results: the curve for $b = 10^{-2}$ closely approaches the dotted line corresponding to Case IV at $\epsilon_0 = 1.0$. For the kinetic system chosen the largest practical value of b was estimated to be 10^{-3} (Table 2). Hence the stationary state hypothesis seems likely to be satisfactory for real systems represented by kinetics of Equations (1) to (3).

The dotted lines in Figure 2 show the effect of ϵ_0 under the restrictions of the stationary state hypothesis. Comparison with the dashed curve for $\epsilon_0 \to 0$ shows that there is a negligible effect of ϵ_0 below at 10^{-1}. The increase in conversion to product B with decreasing ϵ_0 may seem strange. However, b also depends upon α and is a measure of I_0. The pertinent factor measuring the effect of I_0 on conversion is the ratio of the rate of incident radiation to the feed rate of reactant, or

$$\frac{I_0(2\pi RL)}{C_{A_0} v \pi R^2} = \frac{2b\theta_0}{\varphi\epsilon_0} \text{ Einsteins/g. mole}$$

This can be conveniently expressed as the dimensionless intensity per unit concentration of reactant, or

$$2\beta = \frac{2b\theta_0}{\epsilon_0} \tag{34}$$

Since $ab\theta_0 = 1$ and $a = 1$ in Figure 2, $b\theta_0$ is constant. Equation (34) shows that β increases as ϵ_0 decreases. Hence the conversion to B should increase as ϵ_0 decreases.

The decrease in Z with increasing b in Figure 2 may also seem strange, because b is an effective rate constant for the initialtion step. However, the restriction of constant a and $ab\theta_0$ means that τ_0 and k_2 also decrease as b increases.

Figure 3 is similar to Figure 2 except that, $a = 0.1$, and only the results for $\epsilon_0 \to 0$ (Cases IIIa and IVa) are included. At this lower a value, Y becomes a function of b, while for $a = 1$ in Figure 2 there is but one Y curve for all b. The results in Figure 3 again show that the stationary state hypothesis is satisfied after the first section of the reactor at $b \leq 1.0^{-3}$. Comparison of the curves of X, Y, Z in Figures 2 and 3 shows that as a decreases (corresponding to an increase in k_3), the induction period and the extent of deviation from the stationary state both decrease.

Radial Concentration Profiles

The solutions for Cases I and II show radial concentration profiles of product B for different levels of diffusion (M values). These are illustrated in Figures 4 and 5 for $ab\theta_0 = 1$, $a = 1$ and $b = 0.1$ for a position near the reactor entrance ($\zeta = 0.25$), and at the exit ($\zeta = 1.0$). The results in Figure 4 (plug flow) suggest that $M = 10$ is

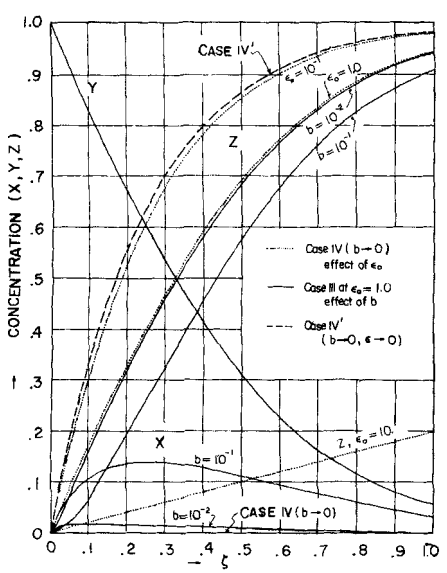

Fig. 2. Effect of kinetic constants and ϵ_0 for Case III, ($a = 1$, $ab\theta_0 = 1.0$).

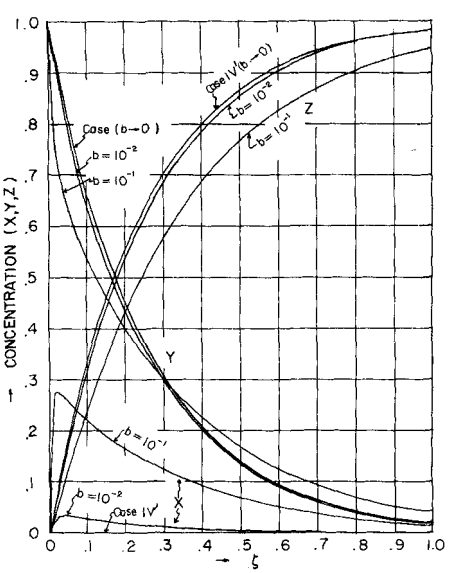

Fig. 3. Effect of kinetic constants at $\epsilon_0 \to 0$ for Case III, ($a = 0.1$, $ab\theta_0 = 1.0$).

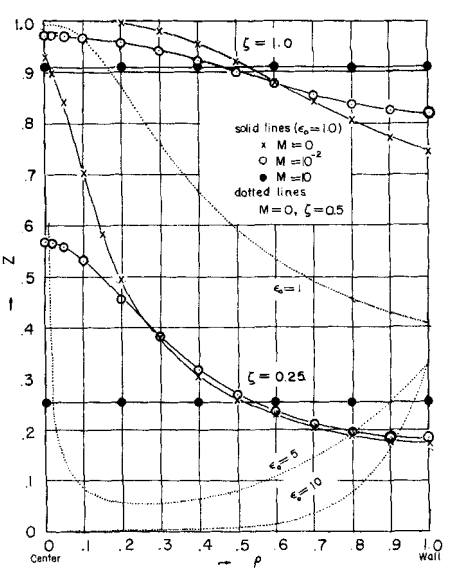

Fig. 4. Radial concentration profile of Z for Case II, $ab\theta_0 = 1$, $a = 1$, $b = 0.1$.

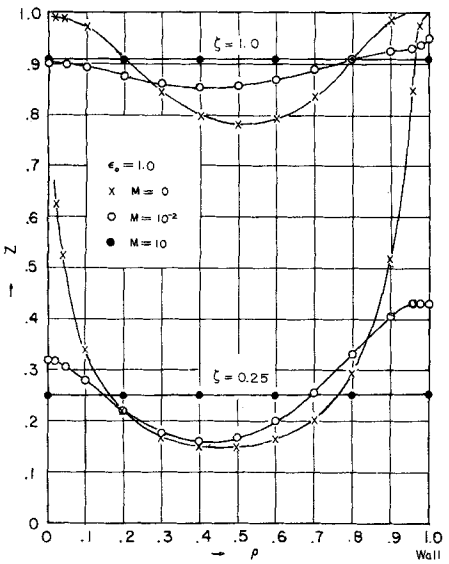

Fig. 5. Radial concentration profile of Z for Case I, $ab\theta_o = 1.0$, $a = 1$, $b = 0.1$.

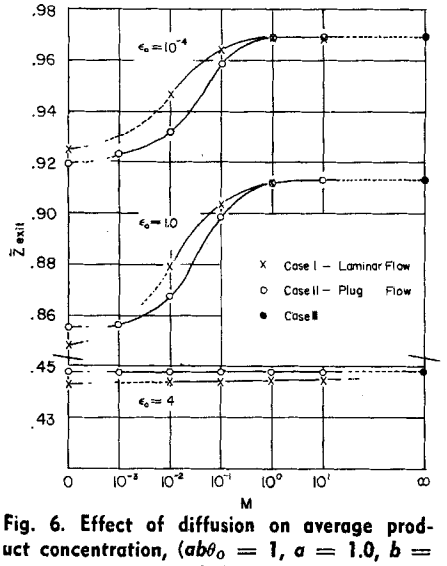

Fig. 6. Effect of diffusion on average product concentration, ($ab\theta_o = 1$, $a = 1.0$, $b = 0.1$).

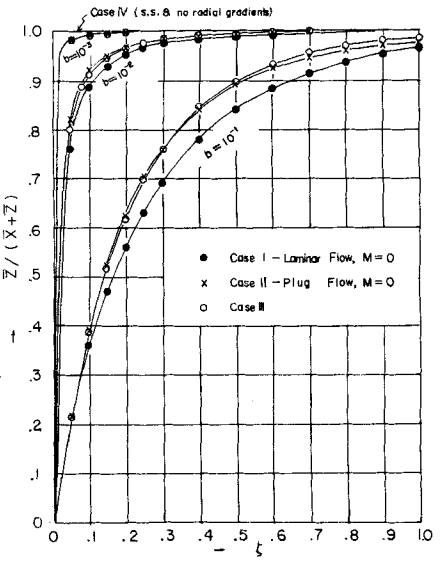

Fig. 7. $\bar{Z}/(\bar{X}+\bar{Z})$ vs. ζ for different reactor models, $ab\theta_o = 1$, $a = 1$.

high enough for the concentration profile to be nearly flat. At lower M, profiles develop and correspond to higher concentrations of product near the center. This reflects the effect of the converging radiation to a higher intensity near the axis. Note that for a conventional plug flow reactor, radial gradients would not exist.

Comparison of Figures 4 and 5 illustrates the effect of the laminar velocity profile. The profiles for laminar flow (Fig. 5) exhibit a minimum caused by the counteracting effects of the light intensity and velocity profiles. The former increases the rate of reaction near the axis, and the latter increases the residence time near the wall. Both cause Z to increase.

The dotted lines in Figure 4 describe the significance of the optical thickness ϵ_o on the profiles for no diffusion, $M = 0$, midway along the reactor, ($\zeta = 0.5$). The general effect of increasing product concentration as ϵ_o decreases was observed in Figure 2 and is due to a larger β [see Equation (34)]. At low ϵ_o, the radiation passes through the reactor with little absorption. This results in higher rates of reaction near the tube center and a rising profile toward the center, as illustrated by the dotted line for $\epsilon_o = 1$. At high ϵ_o, not much light is transmitted so that the intensity is greatest at the wall. It is again high, for geometrical reasons, very close to the center. These factors cause the concentration of product to rise both near the wall and near the center, as shown by the curve for $\epsilon_o = 5$.

Effect of Radial Diffusion

The effect of the profiles shown in Figures 4 and 5 on the average concentration of product is illustrated in Figure 6. Again $ab\theta_o = 1$, $a = 1.0$ and $b = 0.1$. For the laminar flow reactor the product concentration increases with M in the range 10^{-3} to 10^{-1} but flattens out above 10^{-1}, approaching the maximum result, corresponding to Case III. This increase is in agreement with conventional, laminar flow reactor performance (7). The plug flow photoreactor, Case II, exhibits the same general effect of M in contrast to a conventional plug flow reactor for which no influence of M would be possible.

At low ϵ_o the product concentration is higher for laminar flow while at high ϵ_o the situation is reversed. It appears that the normal disadvantage of a laminar flow reactor due to short residence time near the center of the tube is offset by the higher light intensity. At high ϵ_o, the radiation does not reach the center so that the high intensity is not achieved, and the relation between laminar and plug flow operation is the usual one.

Axial Profile and Stationary State Hypothesis

Cassano and Smith (6) interpreted photochlorination data in a laminar flow reactor by assuming stationary state kinetics and neglecting radial diffusion. Since their results were for low conversions (differential reactor operation) radial diffusion was not likely to be important. It is of interest to know if radial concentration gradients would affect reactor performance in an integral reactor. Two points seem significant: does the criterion of $b \leq 10^{-3}$ for the stationary state hypothesis hold when there are radial gradients (Cases I and II) as well as it did for Case III (see Figure 2), and do radial gradients affect the average product concentration even when the stationary state hypothesis is valid.

Graphs of concentration versus reactor length for different b values provide information on the first question. The ratio $\bar{Z}/(\bar{X} + \bar{Z})$ approaches unity when the stationary state hypothesis is satisfied. Figure 7 shows a plot of this type for $ab\theta_o = 1$ and $a = 1$ for Cases I and II with $M = 0$. The results indicate that when $b \leq 10^{-3}$, the stationary state is attained shortly after the entrance to the

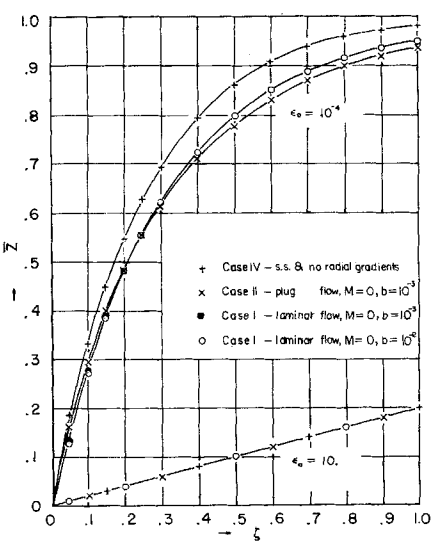

Fig. 8. $\bar{Z}$ vs. ζ for different reactor models, $ab\theta_o = 1$, $a = 1$.

reactor, and just as soon for Cases I and II as for Case III. Hence the $b \leq 10^{-3}$ criterion appears to be a valid one for the laminar flow reactor, for the kinetic system chosen.

Figure 8 compares $\overline{Z}$ vs. ζ curves at $b = 10^{-3}$ for the different cases. For low optical thicknesses ($\epsilon_o = 10^{-4}$) the curves for Cases I and II are lower than that for the stationary state case with no radial gradients. For high ϵ_o ($\epsilon_o = 10$) the radiation is absorbed near the outer wall and the effects of radial gradients on the average product concentration are negligible. Hence the answer to the second question depends upon the level of ϵ_o, but for the important case of low optical thickness, it appears that radial gradients can affect reactor performance even at stationary state conditions.

Effect of Operating Variables on Reactor Performance

The effect of an increase in a single variable, for example light intensity I_o, on the concentration of product is difficult to visualize because of the number of, and the interaction between, the dimensionless parameters. To clarify this, Table 3 shows the effect, in the fourth column, on Z of an increase in the variable given in the first column. The second and third columns give the parameters that must vary and remain constant to give the desired effect.

The results in Table 3 are illustrated in Figure 9 where Z is plotted vs. ϵ_o at constant β, a, and θ_o for Case III. From the table the variation with ϵ_o under these conditions shows the effect of the absorptivity α. According to the table, the effect of intensity also can be obtained by comparing curves at the same ϵ_o but different β; for example, points A, B, C and D for $\epsilon_o = 1.0$ show this effect.

Table 3. The Effect of Operating Variables on Product Concentration Z*

Variable (which increases)	Design parameters vary	Design parameters constant	Effect on Z
C_{A_o}	ϵ_o (+)†	$ab\theta_o$, a, b, M	decrease
τ_o	θ_o (+) or $ab\theta_o$(+)	a, b, ϵ_o, M	increase
R	M(−) + ϵ_o(+)	$ab\theta_o$, a, b, $M(\epsilon_o)^2$	decrease
α	b(+) + ϵ_o(+)	a, θ_o, β, M	increase
I_o	b(+) or $ab\theta_o$(+)	a, θ_o, ϵ_o, M	increase
$\tau_o + k_3$	a(−)	$ab\theta_o$, b, ϵ_o, M	increase or decrease
$\tau_o + k_2$	b(−)	$ab\theta_o$, a, ϵ_o, M	increase
k_2	a(+) or $ab\theta_o$(+)	b, θ_o, ϵ_o, M	increase

* Results are independent of velocity profile.
† (+), (−) indicates direction of variation.

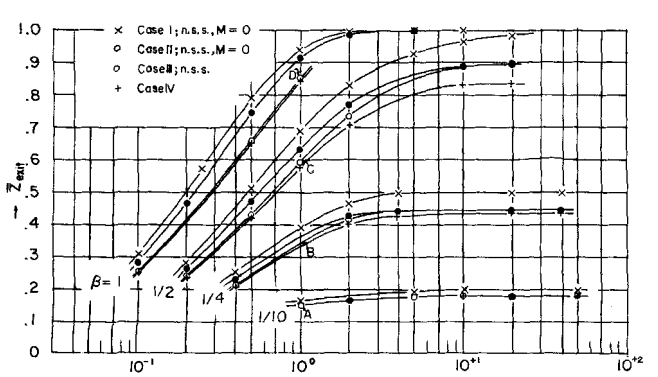

Fig. 9. Effect of ϵ_o on Z at constant β ($a = 1$, $\theta_o = 10$).

CONCLUSIONS

Equations were developed for the concentrations in a tubular photoreactor for first-order termination and propagation (nonchain) kinetics. Four reactor models were considered: laminar flow (Case I), plug flow (Case II), complete radial mixing (Case III), and complete radial mixing plus stationary state kinetics (Case IV). The dimensionless parameters which determined the performance of the reactor were identified; of particular significance are the optical thickness, $2\epsilon_o$, the ratio of initiation to propagation plus termination rate constants, b, and a parameter $ab\theta_o$ which is proportional to the mean residence time and the rate constant for the product reaction. The results showed that:

1. The necessary and sufficient condition for the stationary state hypothesis to be satisfied is $b \leq 10^{-3}$, regardless of the reactor model. Estimates of likely values of rate constants suggest that the stationary state criterion will be met for real systems obeying the chosen kinetics.
2. Even at stationary state conditions, radial diffusion may affect the conversion to product for realistic calues of the diffusion parameter (M) and the optical thickness.

ACKNOWLEDGMENT

The financial support of the Federal Water Pollution Control Administration WP-00952 is gratefully acknowledged. The authors also express their appreciation to the Computer Center of the University of California at Davis and to the National Institutes of Health whose Grant FR-00009 made the computer facilities available.

NOTATION

a = relative rate constant, k_2/d
b = rate parameter for initiation step, κ/d
C = point concentration, g. mole/(cc.)
C_{A_o} = inlet concentration of A, g. mole/(cc.)
D = molecular diffusivity, sq.cm./sec.
d = total rate constant for destruction of unstable intermediate, sec.$^{-1}$
I = point light intensity, Einstein/(sq.cm.)(sec.)
I_o = light intensity at inner wall, Einstein/(sq.cm.)(sec.)
$I(r)$ = net light intensity at radial position r, Einstein/(sq.cm.)(sec.)
$\overline{I}$ = average radial light intensity, Einstein/(sq.cm.)(sec.)
k_2, k_3 = rate constants, sec.$^{-1}$
L = reactor length, cm.
M = diffusion parameter = D^2/dR^2
r = radial distance from axis, cm.
R = radius of reactor, cm.
v = velocity in axial direction, cm./sec.
$\overline{v}$ = average velocity, cm./sec.
X, Y, Z = dimensionless concentrations of A^*, A, B
z = axial distance, cm.

Greek Letters

α = molal absorptivity, sq.cm./g.mole
β = light intensity parameter, $b\theta_o/\epsilon_o$
ϵ_o = one half of optical thickness, $RC_{A_o}\alpha$
ζ = axial distance in reactor, z/L
Ω_i = rate of formation of species i, g.mole/(cc.)(sec.)
θ_o = modified contact time, $\tau_o d$
θ = modified average contact time at ζ, $\theta_o\zeta$
κ = rate constant of initiation step based on light intensity at inner wall, $\varphi\alpha_A I_o$
μ = attenuation coefficient, $\alpha_A C_A$, cm.$^{-1}$
ρ = radial distance, r/R

τ_0 = average residence time = $L/\bar{v}$
φ = quantum yield of initiation step, g.mole/(Einstein)

Subscripts

i = component
r = radial distance
z = axial distance

LITERATURE CITED

1. Benson, S. W., "The foundation of Chemical Kinetics" Butterworth's (1963).
2. ———, *J. Chem. Phys.*, **20**, 1605 (1962).
3. Benson, S. W., *Advan. Photochemistry*, **2**, 1 (1964).
4. Bruce, G. H., D. M. Peaceman, H. H. Rachford, Jr., and J. D. Rice, *Am. Inst. Mining Met. Engrs., Petroleum Trans.* **198**, 79 (1953).
5. Calvert, J. G., and J. N. Pitts, Jr., "Photochemistry," John Wiley, New York (1966).
6. Cassano, A. E., and J. M. Smith, *AIChE J.*, **12**, 1124 (1966).
7. Cleland, F. A., and R. H. Wilhelm, *ibid.*, **2**, 489 (1956).
8. Crank, J., and P. N. Nicholson, *Proc. Cambridge Phil. Soc.*, **43**, 50 (1947).
9. Doede, C. M., and C. A. Walker, *Chem. Eng.* **62**, 159 (1959).
10. Foraboshi, F. P., *Chem. Ind. (Milan)*, **41**, 731 (1959).
11. Gaertner, R. F., and J. A. Kent, *Ind. Eng. Chem.*, **50**, 1223 (1958).
12. Hill, F. B., and R. M. Felder, *AIChE J.*, **11**, 873 (1965); Hill, F. B., and N. Reiss, paper presented at 16th Annual Canadian Chem. Eng. Conference, Windsor, Ontario (Oct. 1966).
13. Huff, J. E., C. A. Walker, *AIChE J.*, **8**, 193 (1962).
14. Lapidus, L., "Digital Computation for Chemical Engineers," McGraw-Hill, New York (1962).
15. Ravinovitch, B. S., and D. W. Setser, *Advan. Photochemistry*, **3**, 1 (1964).
16. Schechter, R. S., and E. H. Wissler, *Appl. Sci. Res., Sect. A:* **9**, 334 (1960).

Manuscript received September 16, 1967; revision received October 12, 1967; paper accepted October 16, 1967.

The Dynamic Behavior of a Packed Liquid Extraction Column

JOSEPH E. DONINGER

International Minerals and Chemical Corporation, Libertyville, Illinois

and WILLIAM F. STEVENS

Northwestern University, Evanston, Illinois

The dynamic behavior of a packed liquid extraction column was investigated by comparing experimental frequency response data obtained from pulse testing with theoretical frequency response data. The theoretical model, which assumed that the column can be represented by a series of perfectly mixed cells, did not adequately describe the frequency response characteristics of the extraction process. However, by the utilization of various magnitude and phase correction factors, a technique was developed to obtain a semiempirical model that could be used to duplicate the actual performance of the liquid extraction column.

In the past few years various attempts have been made to extend the frequency response method of analysis to countercurrent mass transfer operations. Gray and Prados (*9, 10*) have presented a thorough theoretical and experimental investigation of the dynamic behavior of a packed gas absorption column in which carbon dioxide is absorbed from air by water. The frequency response data were obtained by direct sinusoidal forcing of the carbon dioxide input concentration of the gas stream. Several models such as the slug flow, mixing cell, and axial diffusion models were proposed to describe the dynamic behavior of the gas absorption column. Comparison of theoretical and experimental results showed that none of the models completely characterized the gas absorption process. Doninger and Stevens (*3, 4*) proposed that a graphical, semiempirical method be used to describe the frequency response characteristics of a packed gas absorption column.

The first application of arbitrary pulse forcing techniques to obtain frequency response data for chemical engineering processes was made by Lees and Hougen (*13*) in the study of heat exchanger dynamics. Hougen and Walsh (*11*) extended the use of this technique to determine the dynamic behavior of pneumatic control systems, heat exchangers, differential refractometers, and liquid mixing vessels. Watjen and Hubbard (*18, 19*) investigated the dynamics of liquid extraction for a pulsed plate extraction column in which methyl isobutyl ketone was used to extract acetic acid from water. The mass transfer and fluid flow dynamics were excited by injecting a rectangular pulse of acid of short duration into the water phase above the top plate of the column. Samples of the raffinate were taken until the column returned to steady state conditions. The raffinate samples were analyzed by titration and the transient response data were reduced to frequency response data by numerical integration using rectangular area approximation methods. Experiments were also conducted in which only the fluid flow dynamics were excited. The experimental results in the mixer-settler flow region of low column pulse frequency were found to be in good agreement with the linear model theory.

It was the work of Watjen and Hubbard (*18, 19*) which suggested the application of the pulse forcing technique to determine the dynamic behavior of the liquid extraction column. It was felt, however, that an improvement could be made in the type of concentration pulse used to excite the mass transfer dynamics and in the approximation methods used for data reduction. In Watjen's pulse experiments, 2 cc. of pure acetic acid were injected into the system over a period of 1 sec. This caused a high instantaneous concentration of acid in the aqueous phase above the top plate of the column. In the pulse experiments conducted in this study, a rectangular acetic acid pulse with a longer duration but lower concentration was used to minimize the introduction of non-